COMMUNICATION

Supporting Information

Received 00th January 20xx,
Accepted 00th January 20xx

DOI: 10.1039/x0xx00000x

Multinary light absorbing semiconductor nanocrystals with diversified electronic and optical properties

Soubantika Palchoudhury,[a,*] Benjamin T. Diroll,[b] Panchapakesan Ganesh,[c] Jessica Cobos,[d] Sohini Sengupta,[a] Jingsong Huang[c,*]

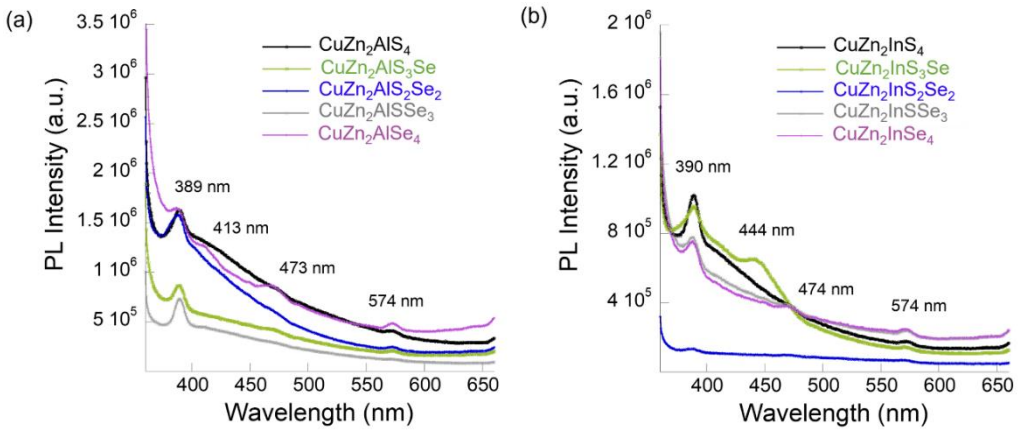

Figure S1. PL characterization of CZASSe nanocrystals for 350 nm excitation. (a) $CuZn_2AlS_xSe_{4-x}$ compositions and (b) $CuZn_2InS_xSe_{4-x}$ compositions.

[a] *Department of Chemical and Materials Engineering, University of Dayton, Dayton, Ohio, USA*
E-mail: spalchoudhury1@udayton.edu
Tel: +1- 937-229-3194
[b] *Center for Nanoscale Materials, Argonne National Laboratory, Lemont, Illinois, USA*
[c] *Center for Nanophase Materials Sciences, Oak Ridge National Laboratory, Oak Ridge, Tennessee 37831, USA.*
E-mail: huangj3@ornl.gov
Tel: +1-865-576-3991
[d] *Mechanical Engineering, University of Texas at El Paso*

† Footnotes relating to the title and/or authors should appear here.
Electronic Supplementary Information (ESI) available: [SEM and EDX analysis of the CZASSe nanocrystals, PL analysis of the $CuZn_2AlSSe$ and $CuZn_2InSSe$ nanocrystals, XRD analysis and Rietveld fit of the CZASSe nanocrystals, experimental bandgap and a table summarizing the bandgaps of CZASSe nanocrystals, and band structure and density of states of the $CuZn_2AlSSe$ and $CuZn_2InSSe$ nanocrystals]. See DOI: 10.1039/x0xx00000x

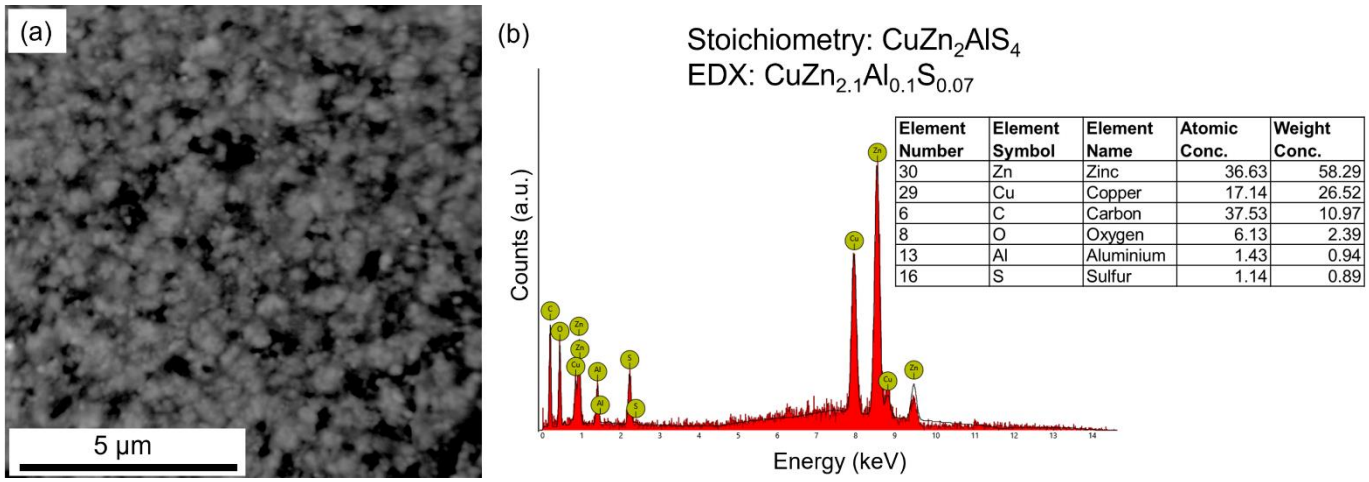

Element Number	Element Symbol	Element Name	Atomic Conc.	Weight Conc.
30	Zn	Zinc	36.63	58.29
29	Cu	Copper	17.14	26.52
6	C	Carbon	37.53	10.97
8	O	Oxygen	6.13	2.39
13	Al	Aluminium	1.43	0.94
16	S	Sulfur	1.14	0.89

Figure S2. SEM and EDX characterization of $CuZn_2AlS_4$ nanocrystals.

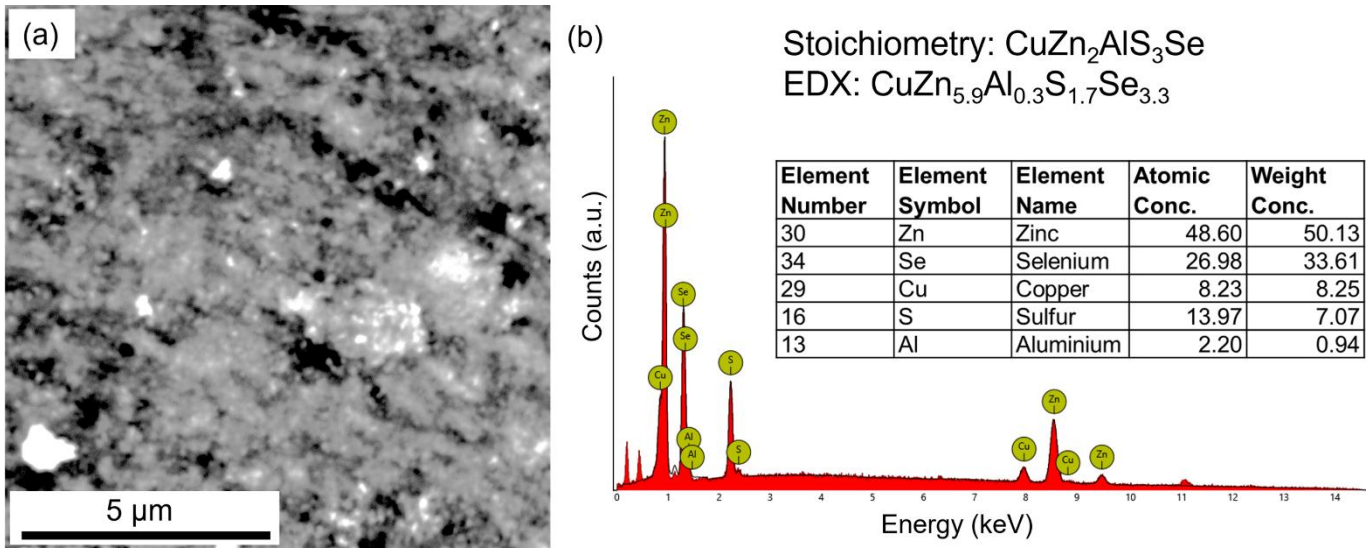

Element Number	Element Symbol	Element Name	Atomic Conc.	Weight Conc.
30	Zn	Zinc	48.60	50.13
34	Se	Selenium	26.98	33.61
29	Cu	Copper	8.23	8.25
16	S	Sulfur	13.97	7.07
13	Al	Aluminium	2.20	0.94

Figure S3. SEM and EDX characterization of $CuZn_2AlS_3Se$ nanocrystals.

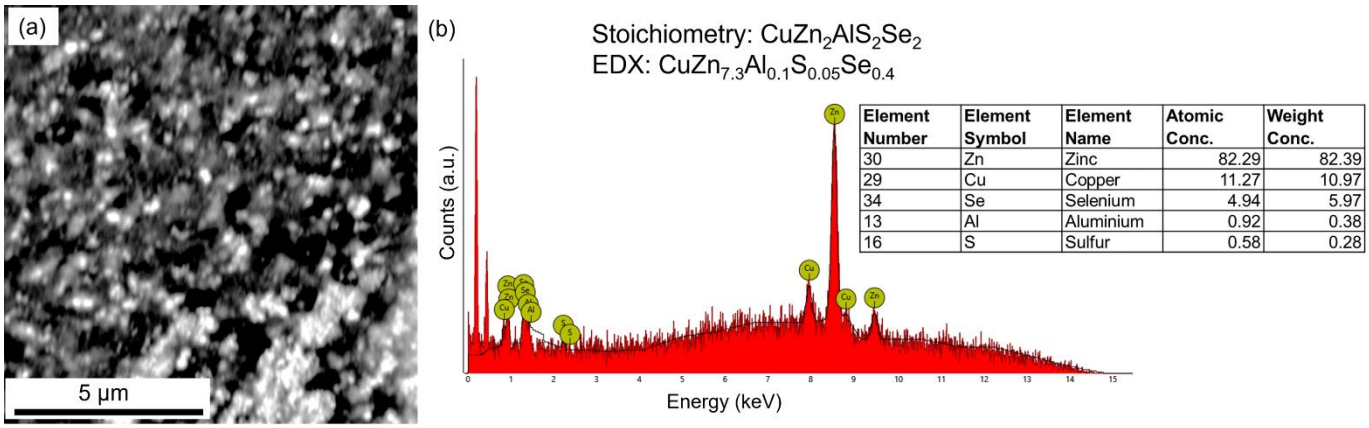

Element Number	Element Symbol	Element Name	Atomic Conc.	Weight Conc.
30	Zn	Zinc	82.29	82.39
29	Cu	Copper	11.27	10.97
34	Se	Selenium	4.94	5.97
13	Al	Aluminium	0.92	0.38
16	S	Sulfur	0.58	0.28

Figure S4. SEM and EDX characterization of $CuZn_2AlS_2Se_2$ nanocrystals.

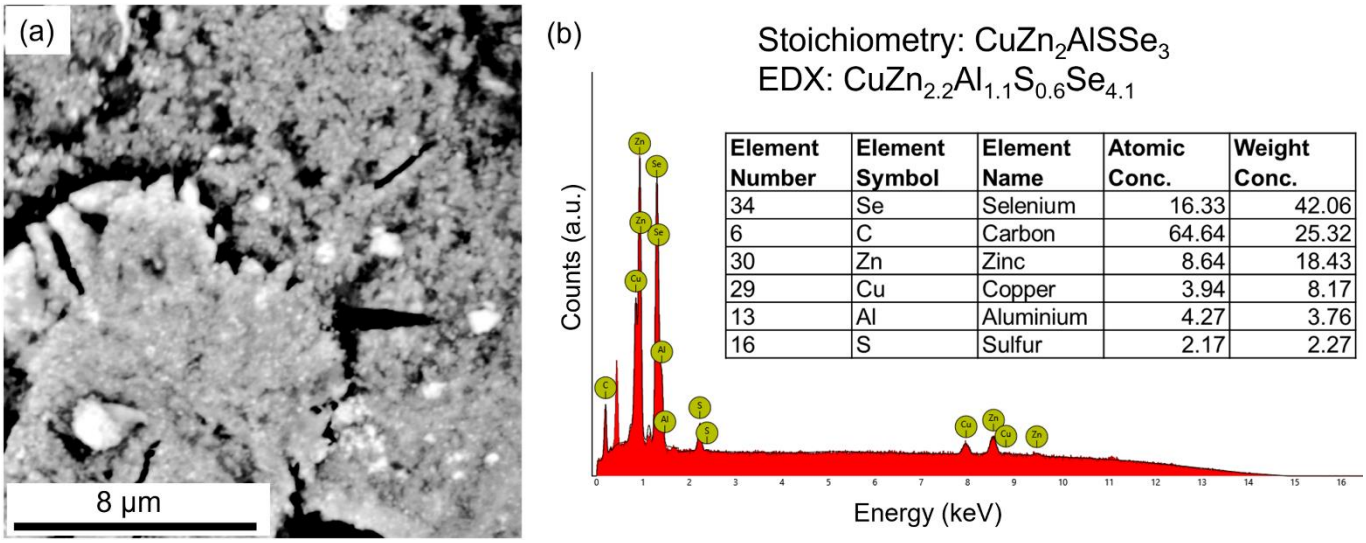

Element Number	Element Symbol	Element Name	Atomic Conc.	Weight Conc.
34	Se	Selenium	16.33	42.06
6	C	Carbon	64.64	25.32
30	Zn	Zinc	8.64	18.43
29	Cu	Copper	3.94	8.17
13	Al	Aluminium	4.27	3.76
16	S	Sulfur	2.17	2.27

Figure S5. SEM and EDX characterization of $CuZn_2AlSSe_3$ nanocrystals.

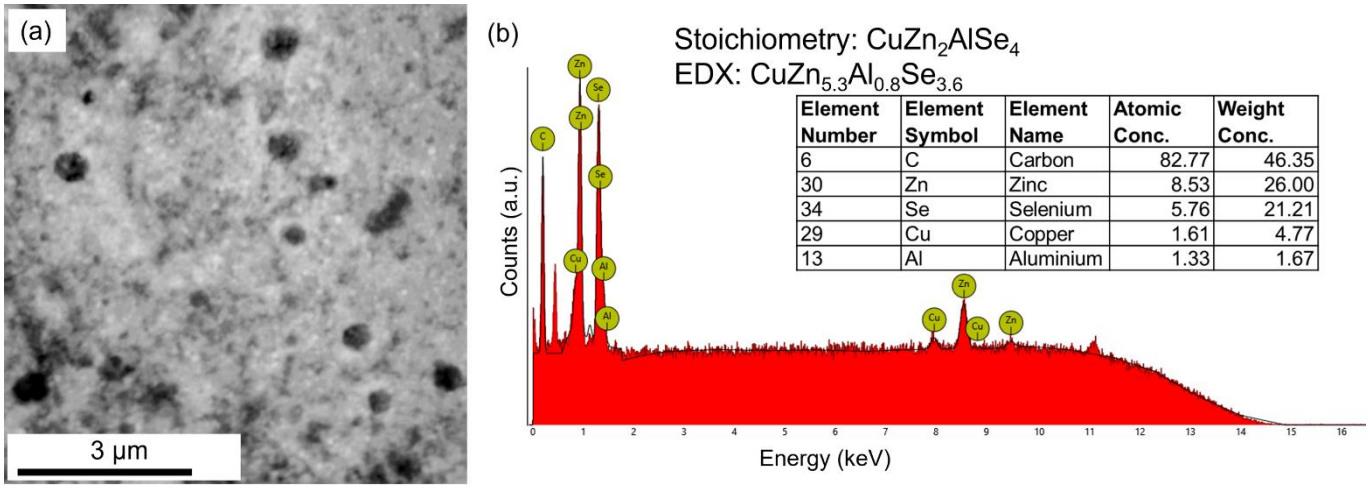

Element Number	Element Symbol	Element Name	Atomic Conc.	Weight Conc.
6	C	Carbon	82.77	46.35
30	Zn	Zinc	8.53	26.00
34	Se	Selenium	5.76	21.21
29	Cu	Copper	1.61	4.77
13	Al	Aluminium	1.33	1.67

Figure S6. SEM and EDX characterization of $CuZn_2AlSe_4$ nanocrystals.

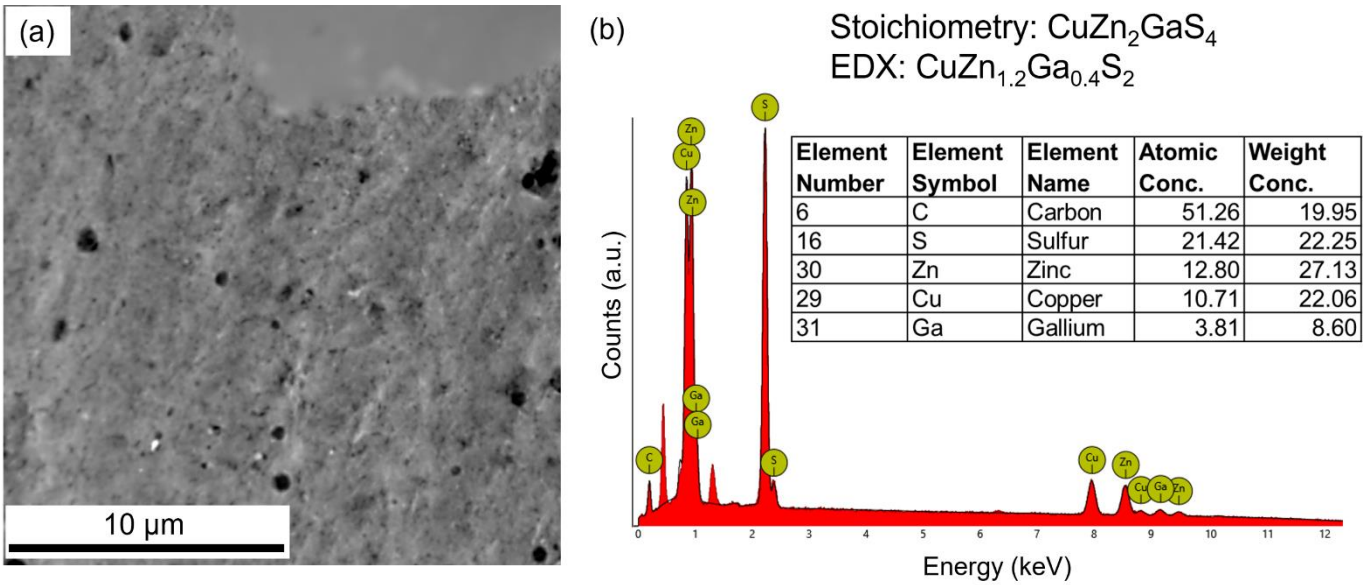

Element Number	Element Symbol	Element Name	Atomic Conc.	Weight Conc.
6	C	Carbon	51.26	19.95
16	S	Sulfur	21.42	22.25
30	Zn	Zinc	12.80	27.13
29	Cu	Copper	10.71	22.06
31	Ga	Gallium	3.81	8.60

Figure S7. SEM and EDX characterization of $CuZn_2GaS_4$ nanocrystals.

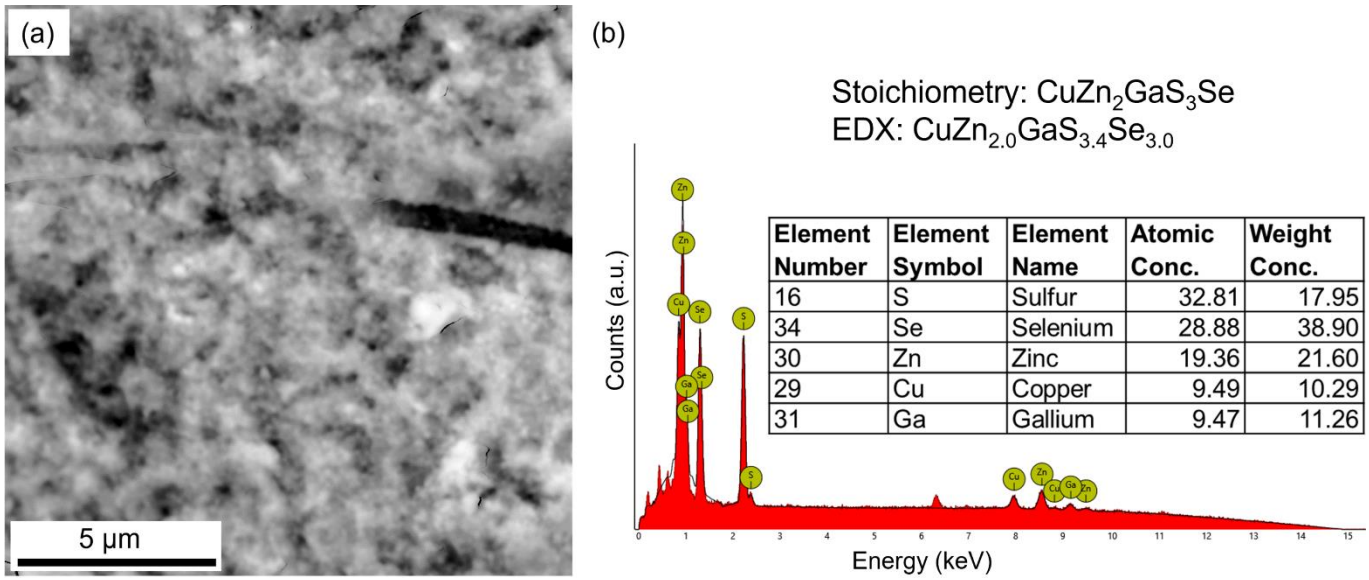

Element Number	Element Symbol	Element Name	Atomic Conc.	Weight Conc.
16	S	Sulfur	32.81	17.95
34	Se	Selenium	28.88	38.90
30	Zn	Zinc	19.36	21.60
29	Cu	Copper	9.49	10.29
31	Ga	Gallium	9.47	11.26

Figure S8. SEM and EDX characterization of $CuZn_2GaS_3Se$ nanocrystals.

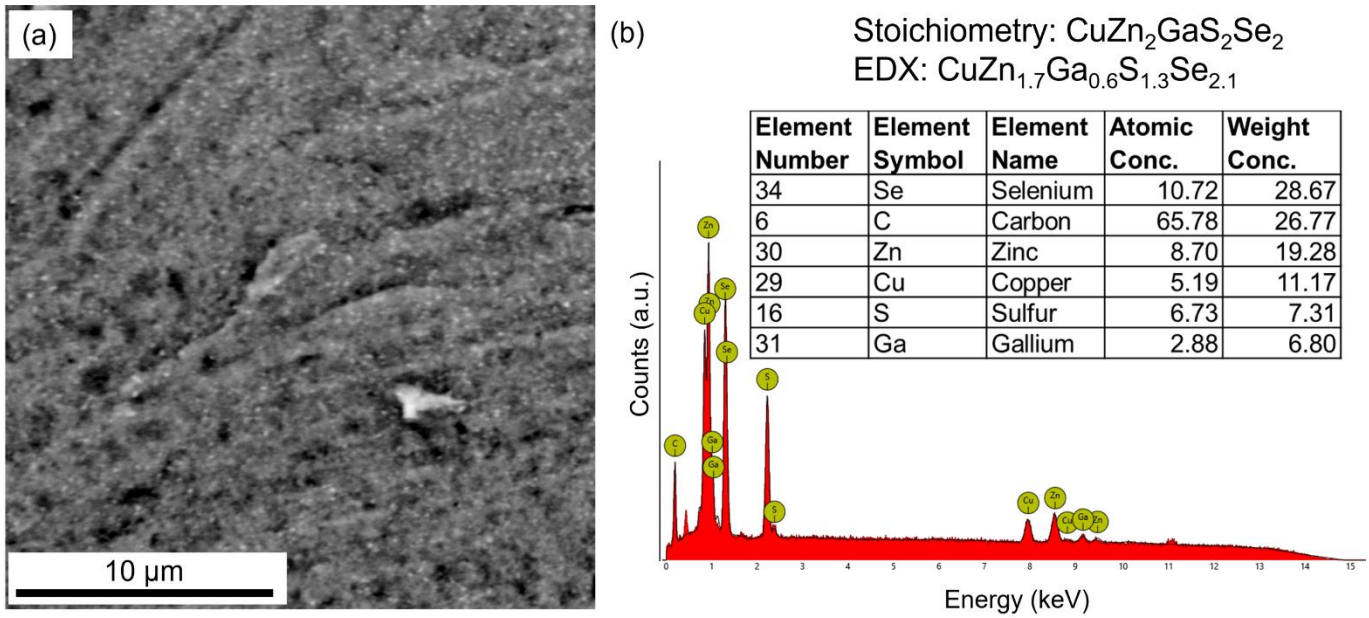

Element Number	Element Symbol	Element Name	Atomic Conc.	Weight Conc.
34	Se	Selenium	10.72	28.67
6	C	Carbon	65.78	26.77
30	Zn	Zinc	8.70	19.28
29	Cu	Copper	5.19	11.17
16	S	Sulfur	6.73	7.31
31	Ga	Gallium	2.88	6.80

Figure S9. SEM and EDX characterization of $CuZn_2GaS_2Se_2$ nanocrystals.

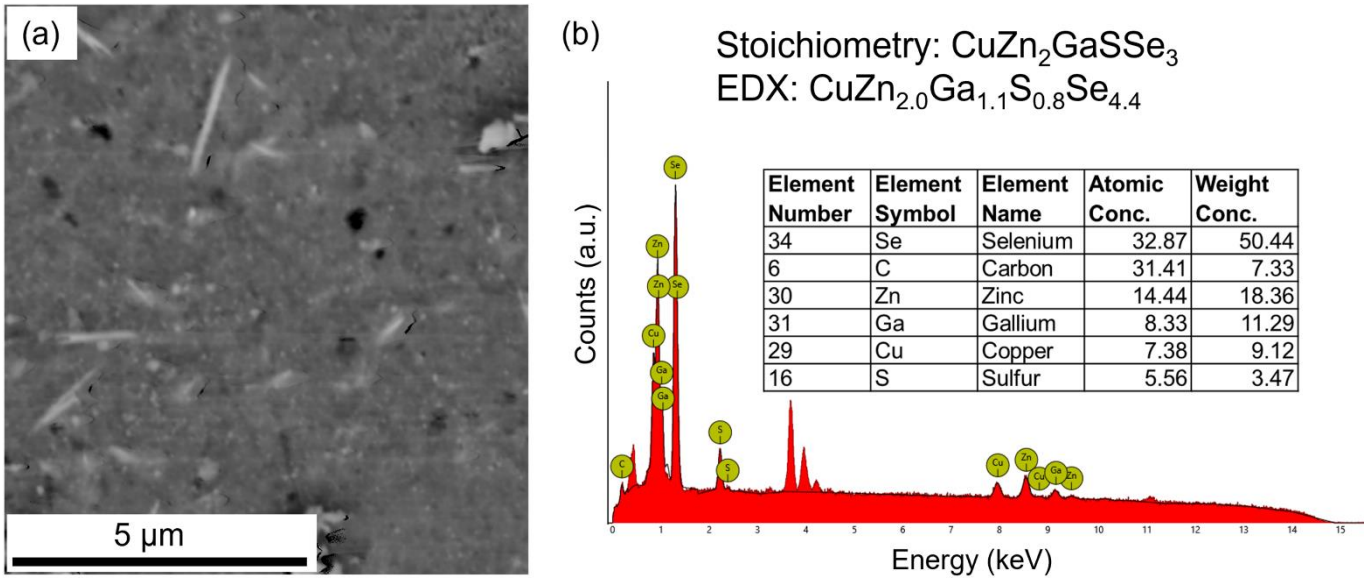

Element Number	Element Symbol	Element Name	Atomic Conc.	Weight Conc.
34	Se	Selenium	32.87	50.44
6	C	Carbon	31.41	7.33
30	Zn	Zinc	14.44	18.36
31	Ga	Gallium	8.33	11.29
29	Cu	Copper	7.38	9.12
16	S	Sulfur	5.56	3.47

Figure S10. SEM and EDX characterization of $CuZn_2GaSSe_3$ nanocrystals.

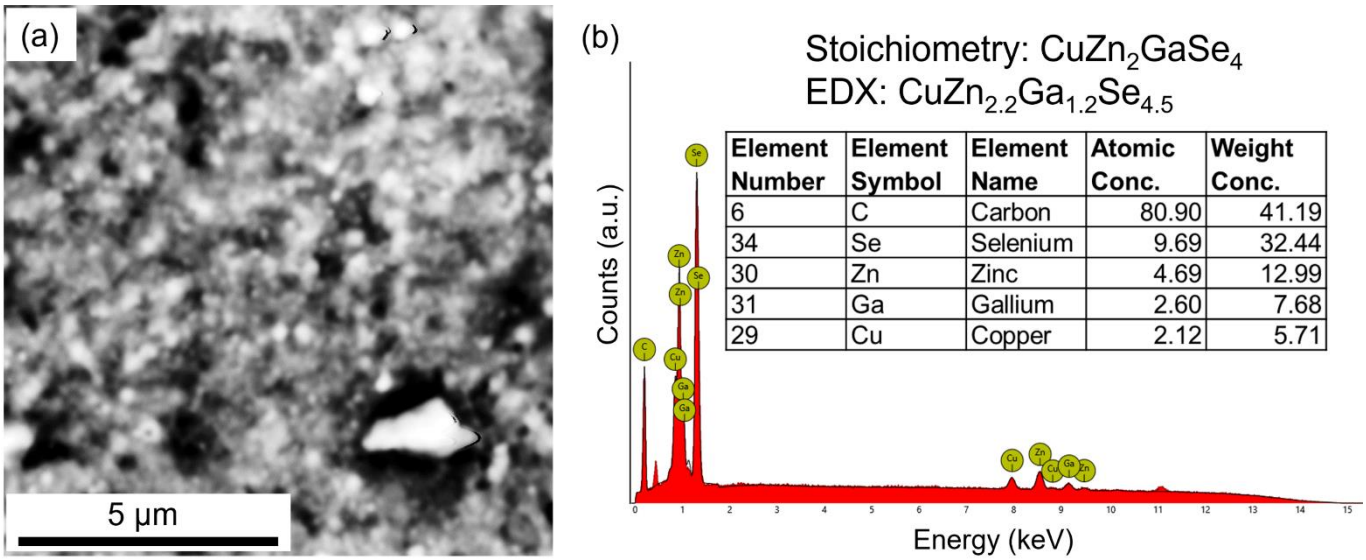

Element Number	Element Symbol	Element Name	Atomic Conc.	Weight Conc.
6	C	Carbon	80.90	41.19
34	Se	Selenium	9.69	32.44
30	Zn	Zinc	4.69	12.99
31	Ga	Gallium	2.60	7.68
29	Cu	Copper	2.12	5.71

Figure S11. SEM and EDX characterization of $CuZn_2GaSe_4$ nanocrystals.

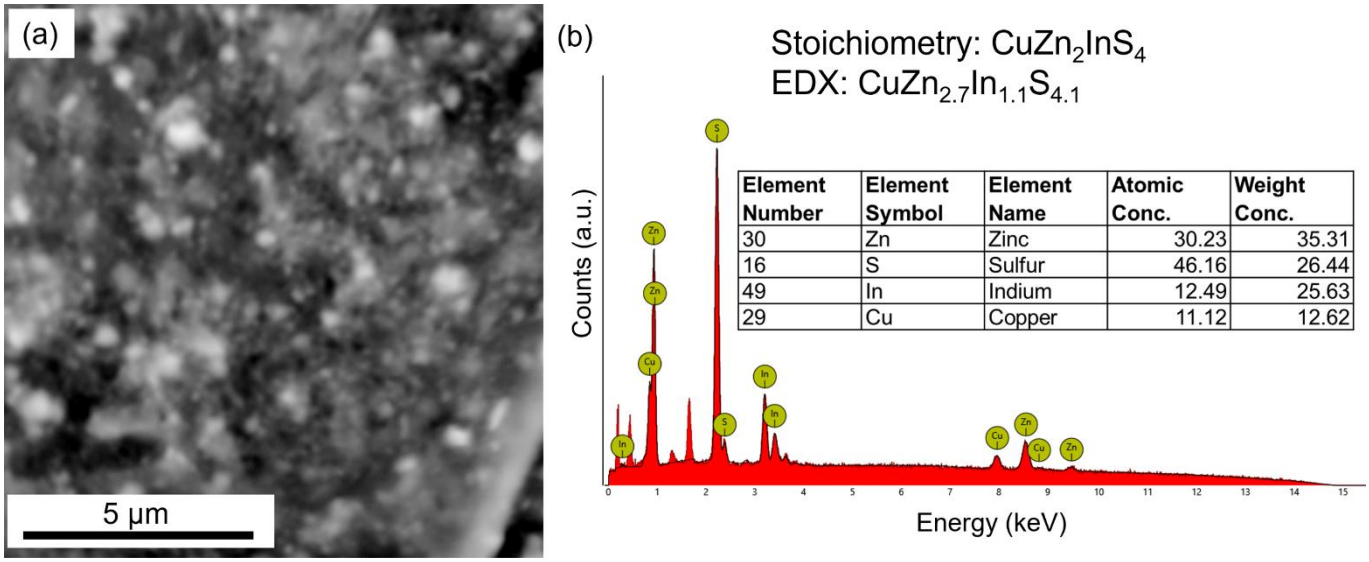

Element Number	Element Symbol	Element Name	Atomic Conc.	Weight Conc.
30	Zn	Zinc	30.23	35.31
16	S	Sulfur	46.16	26.44
49	In	Indium	12.49	25.63
29	Cu	Copper	11.12	12.62

Figure S12. SEM and EDX characterization of $CuZn_2InS_4$ nanocrystals.

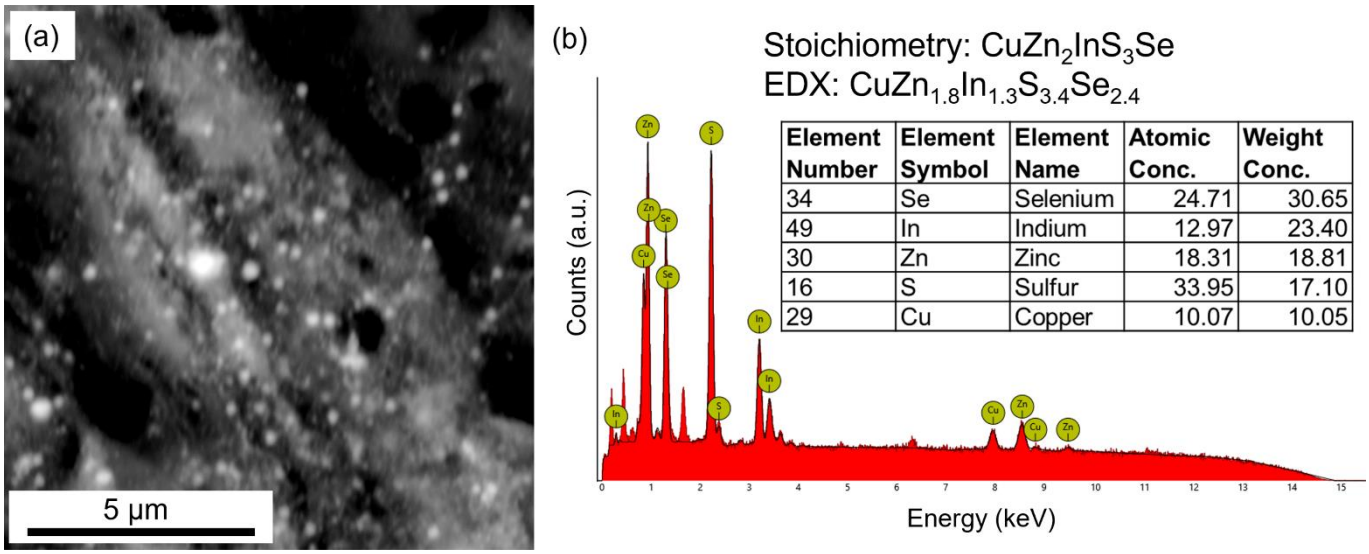

Element Number	Element Symbol	Element Name	Atomic Conc.	Weight Conc.
34	Se	Selenium	24.71	30.65
49	In	Indium	12.97	23.40
30	Zn	Zinc	18.31	18.81
16	S	Sulfur	33.95	17.10
29	Cu	Copper	10.07	10.05

Figure S13. SEM and EDX characterization of $CuZn_2InS_3Se$ nanocrystals.

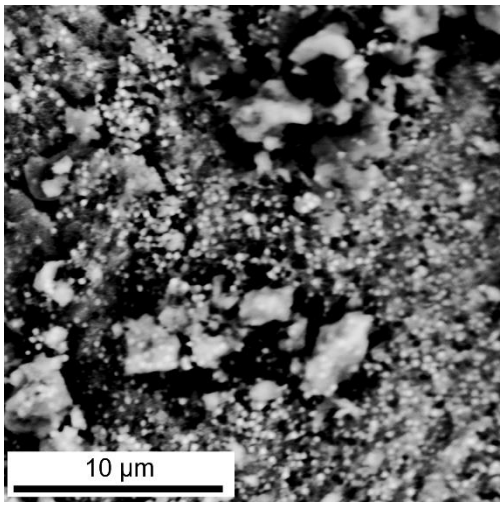

Figure S14. SEM characterization of $CuZn_2InS_2Se_2$ nanocrystals.

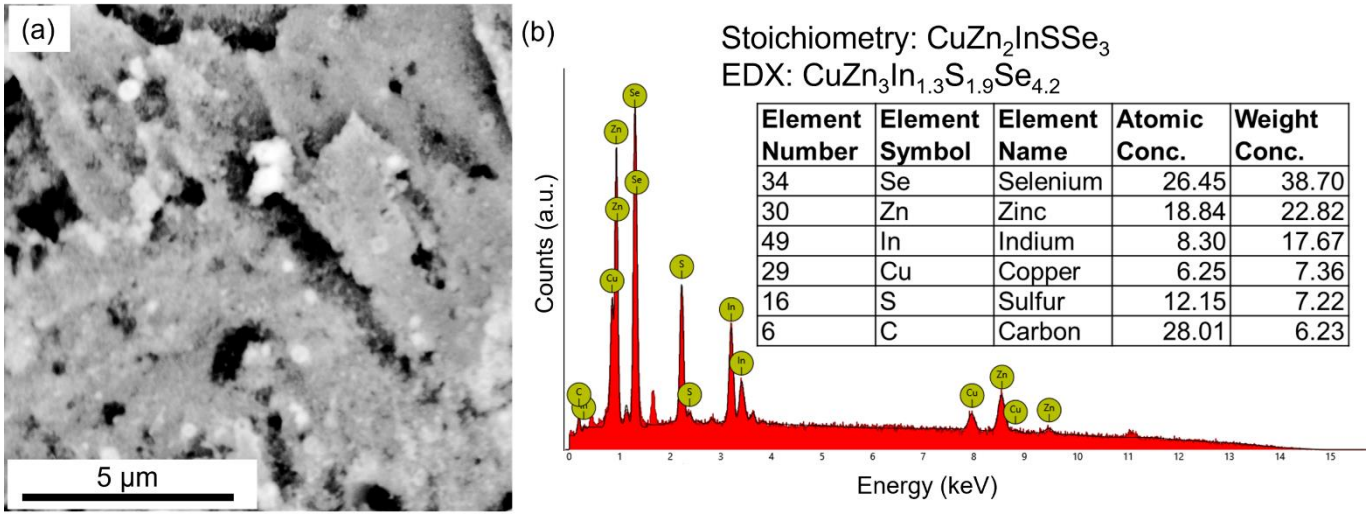

Element Number	Element Symbol	Element Name	Atomic Conc.	Weight Conc.
34	Se	Selenium	26.45	38.70
30	Zn	Zinc	18.84	22.82
49	In	Indium	8.30	17.67
29	Cu	Copper	6.25	7.36
16	S	Sulfur	12.15	7.22
6	C	Carbon	28.01	6.23

Figure S15. SEM and EDX characterization of $CuZn_2InSSe_3$ nanocrystals.

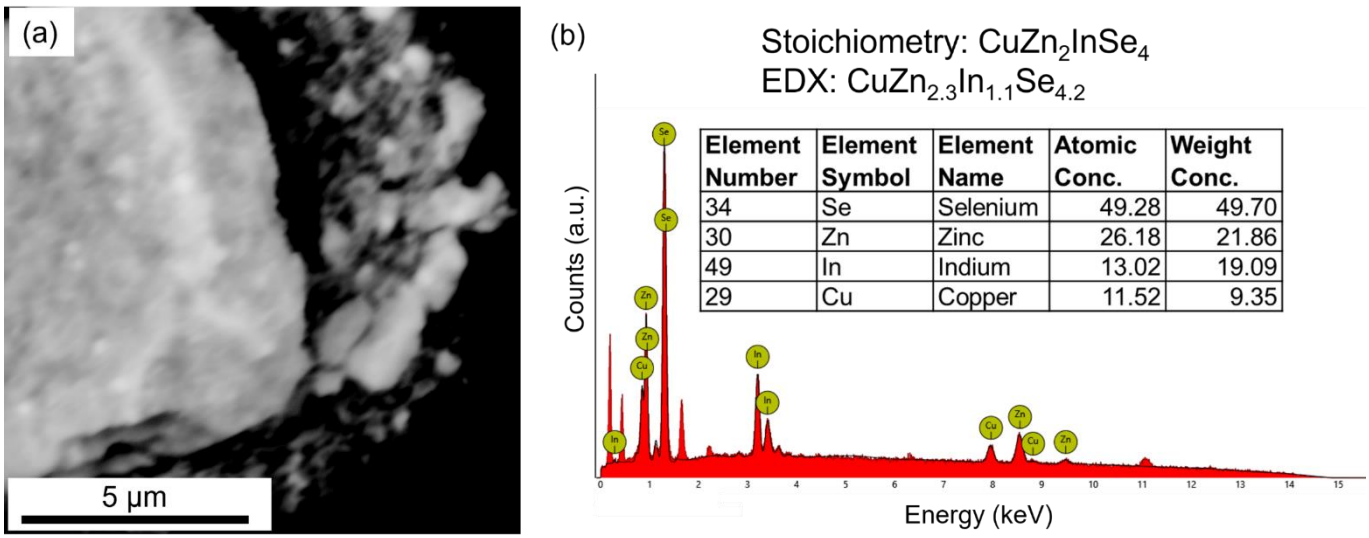

Figure S16. SEM and EDX characterization of $CuZn_2InSe_4$ nanocrystals.

Table S1. Summary of direct experimental bandgaps of CZASSe nanocrystals

Multinary nanocrystal composition	Eg_SCAN (eV)	Eg_HSE06 (eV)	Eg_experimental (eV)	% deviation w.r.t. SCAN	% deviation w.r.t. HSE06	ChemComm Eg_experimental (eV)[1]	Standard deviation	Crystallite size from Debye-Scherrer formula (nm)
$CuZn_2AlS_4$	2.362	3.279	3.0	18.9	3.8	1.78	0.05	23.45
$CuZn_2AlS_3Se$	1.927	2.774	2.2	9.7	9.5			7.58
$CuZn_2AlS_2Se_2$	1.656	2.467	2.4	28.8	11.6			10.93
$CuZn_2AlSSe_3$	1.522	2.342	2.5	36.8	19.8			9.56
$CuZn_2AlSe_4$	1.520	2.369	2.3	31.0	11.1			12.90
$CuZn_2GaS_4$	1.863	2.791	2.2	19.9	8.6	1.64	0.04	4.83
$CuZn_2GaS_3Se$	1.443	2.299	1.8	25.6	1.7			9.87
$CuZn_2GaS_2Se_2$	1.182	2.002	2.5	56.7	36.5			7.66
$CuZn_2GaSSe_3$	1.052	1.880	1.8	46.6	18.2			11.50
$CuZn_2GaSe_4$	1.044	1.903	1.8	46.6	16.5			13.17
$CuZn_2InS_4$	1.214	2.116	2.8	56.2	35.4	1.42	0.03	3.51
$CuZn_2InS_3Se$	0.903	1.733	2.7	66.2	46.7			5.54
$CuZn_2InS_2Se_2$	0.723	1.513	3.0	75.6	58.5			4.80
$CuZn_2InSSe_3$	0.640	1.436	2.4	72.6	51.3			12.68
$CuZn_2InSe_4$	0.650	1.473	2.4	72.3	50.0			18.28

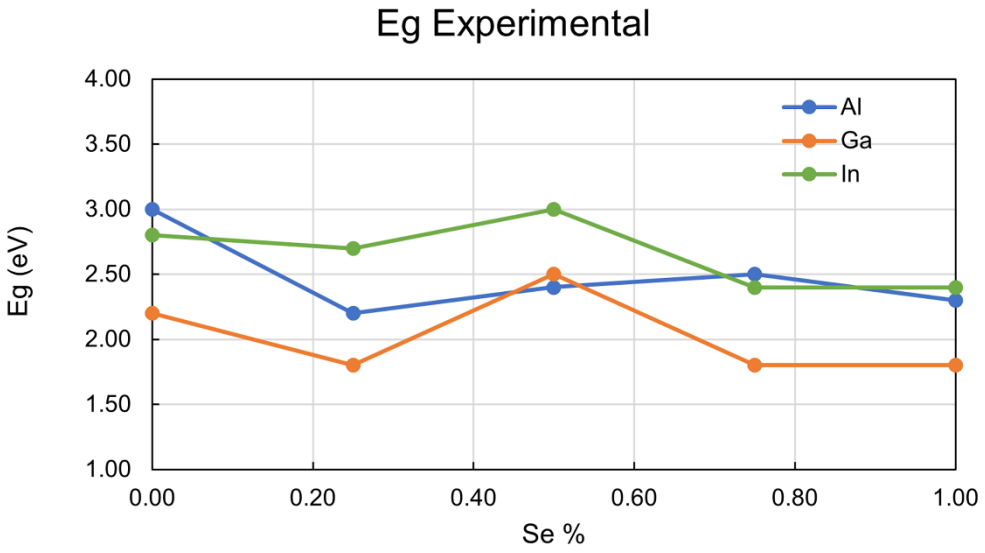

Figure S17. Plot showing variation of experimental bandgap of $CuZn_2AS_xSe_{4-x}$ nanocrystal compositions with varying Se content of the nanocrystals.

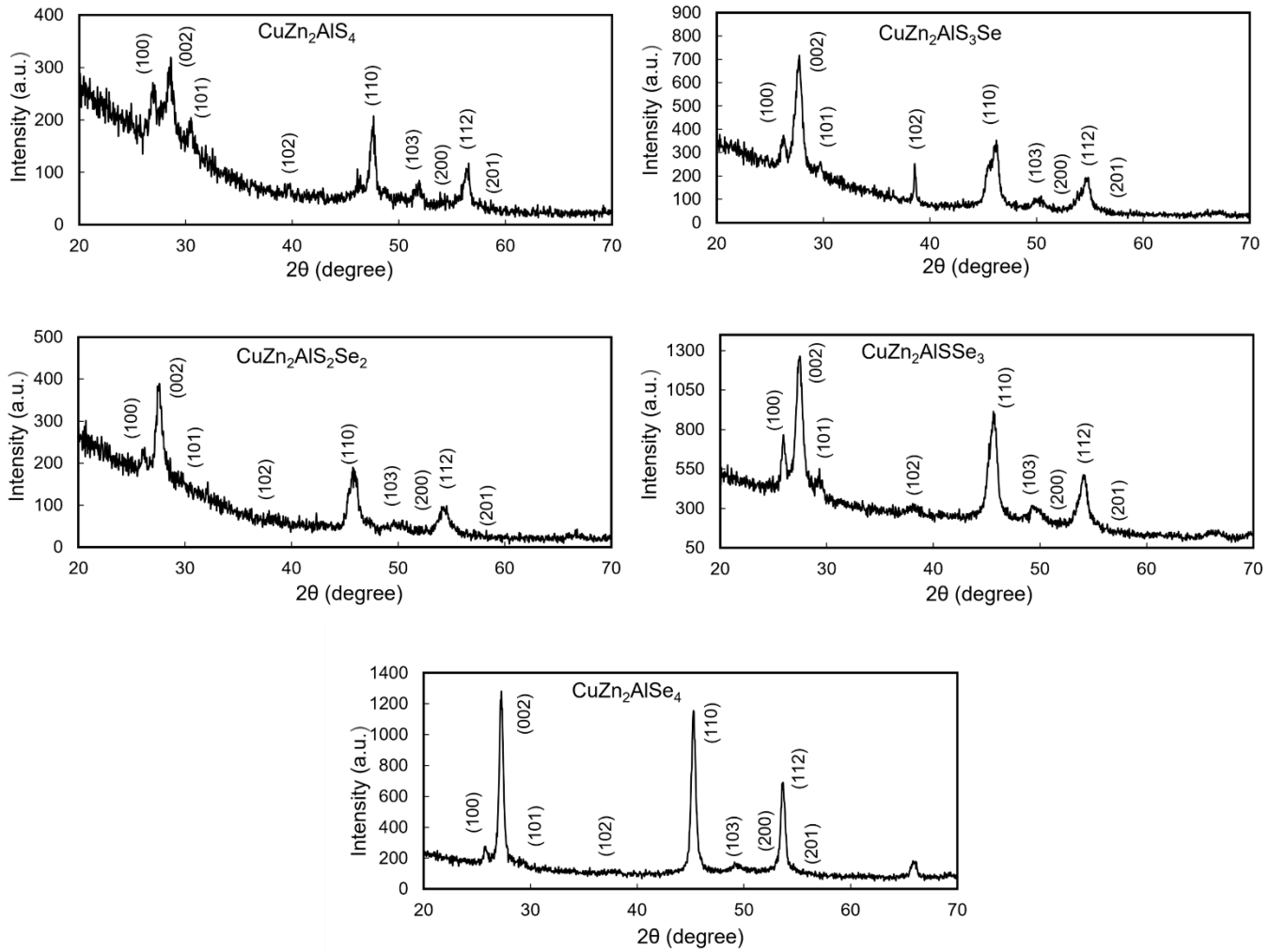

Figure S18. XRD characterization of the different wurtzite phase $CuZn_2AlS_xSe_{4-x}$ nanocrystal compositions.

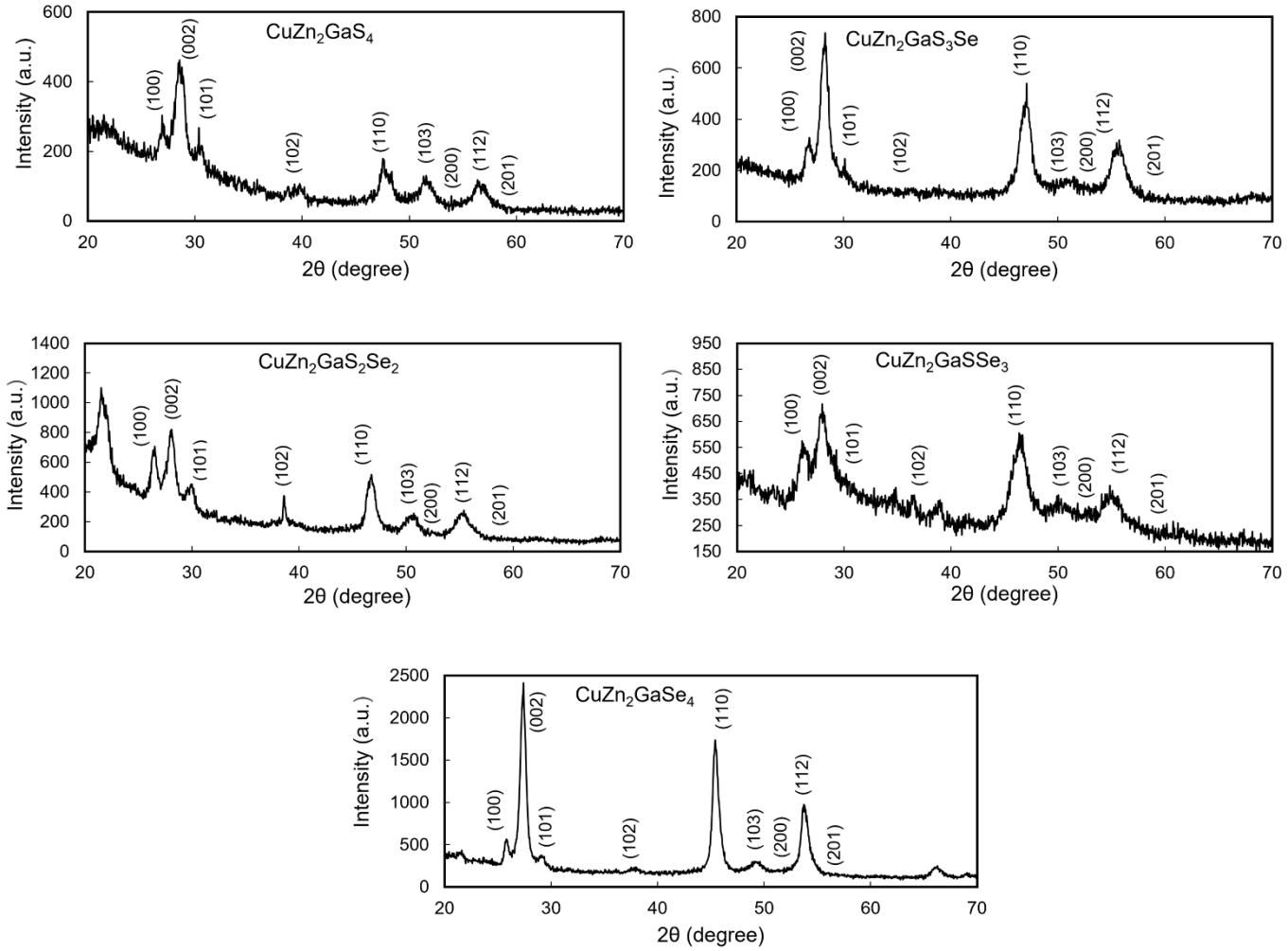

Figure S19. XRD characterization of the remaining wurtzite phase $CuZn_2GaS_xSe_{4-x}$ nanocrystal compositions.

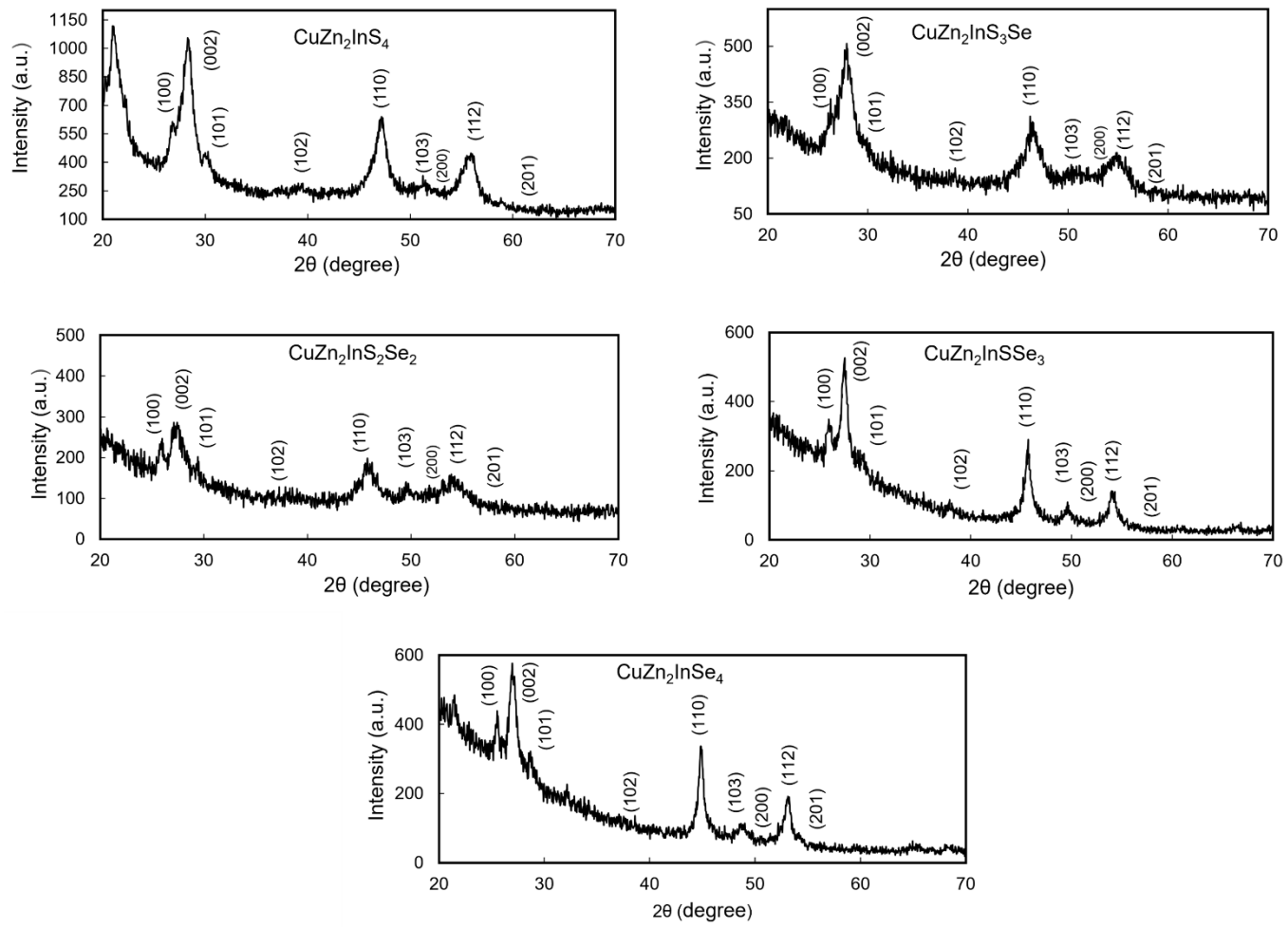

Figure S20. XRD characterization of different wurtzite phase $CuZn_2InS_xSe_{4-x}$ nanocrystal compositions.

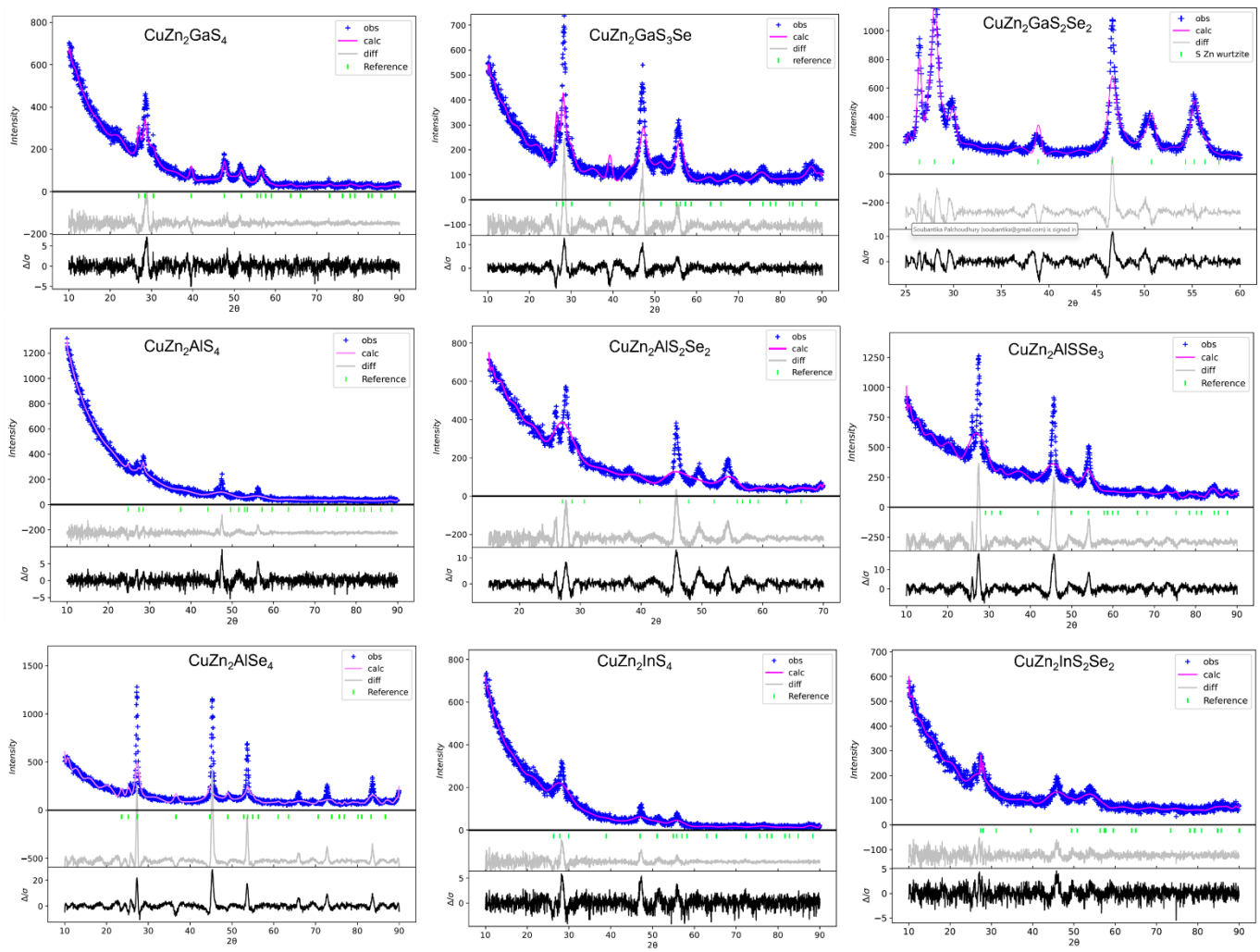

Figure S21. Rietveld fit of different CZASSe nanocrystal compositions.

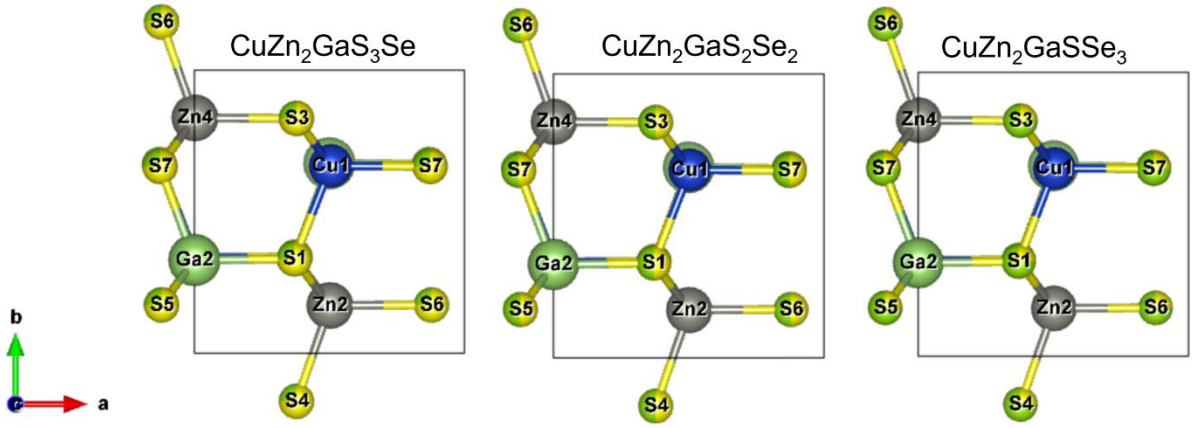

Figure S22. Unit cell of different $CuZn_2GaS_xSe_{4-x}$ compositions used for electronic structure calculations.

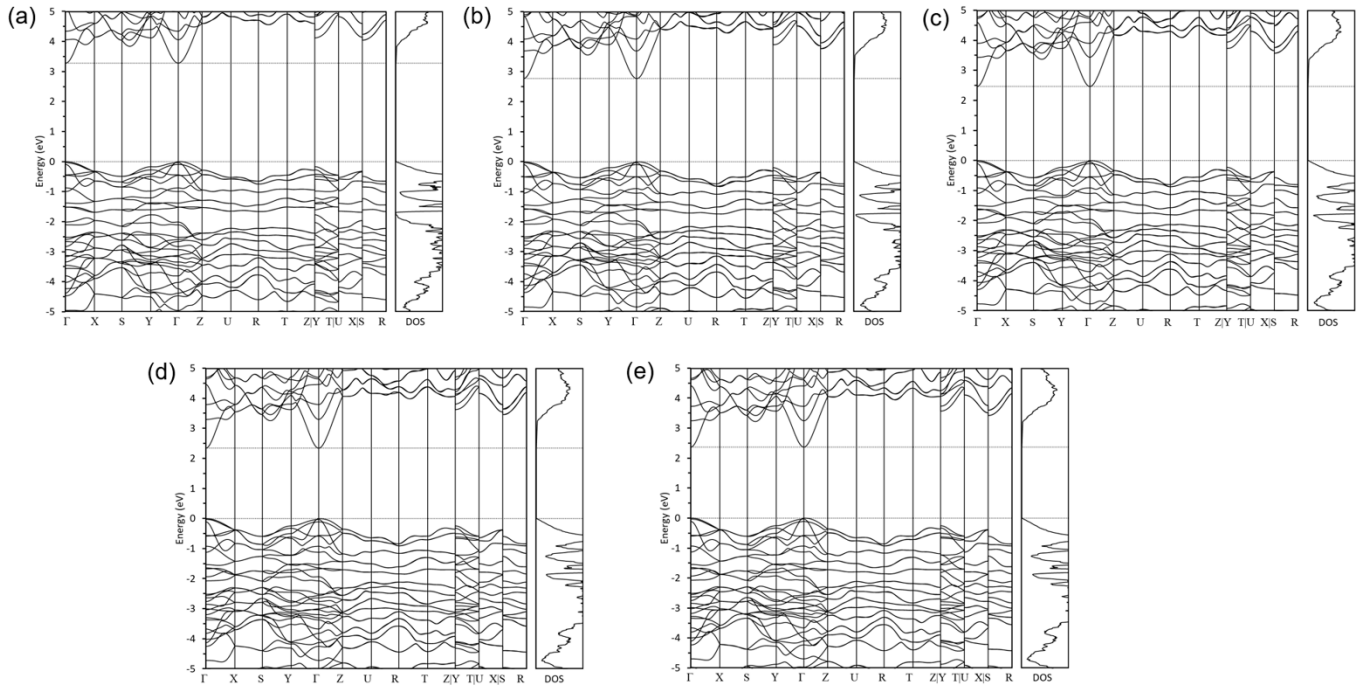

Figure S23. Electronic structures of different $CuZn_2AlS_xSe_{4-x}$ compositions calculated using HSE06 hybrid functionals along with virtual crystal approximation. (a) $CuZn_2AlS_4$, (b) $CuZn_2AlS_3Se$, (c) $CuZn_2AlS_2Se_2$, (d) $CuZn_2AlSSe_3$, and (e) $CuZn_2AlSe_4$.

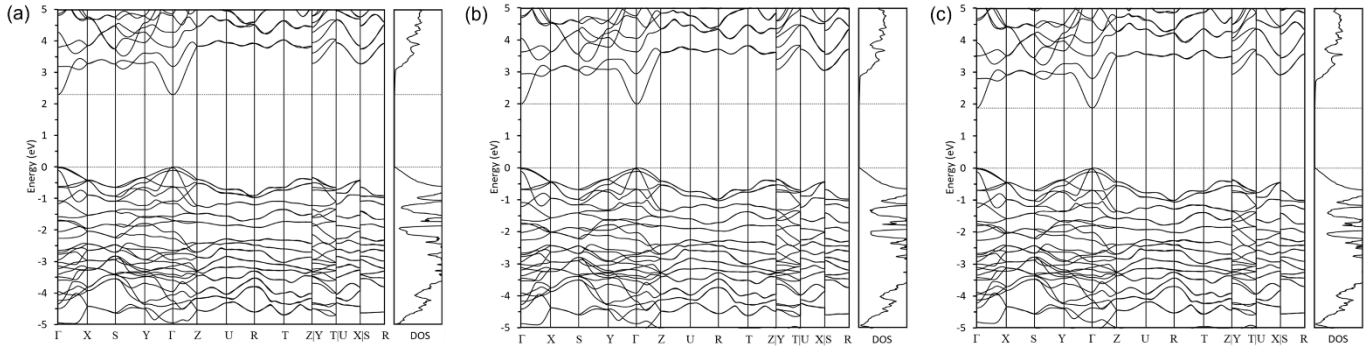

Figure S24. Electronic structures of different $CuZn_2GaS_xSe_{4-x}$ compositions calculated using HSE06 hybrid functionals along with virtual crystal approximation. (a) $CuZn_2GaS_3Se$, (b) $CuZn_2GaS_2Se_2$, and (c) $CuZn_2GaSSe_3$.

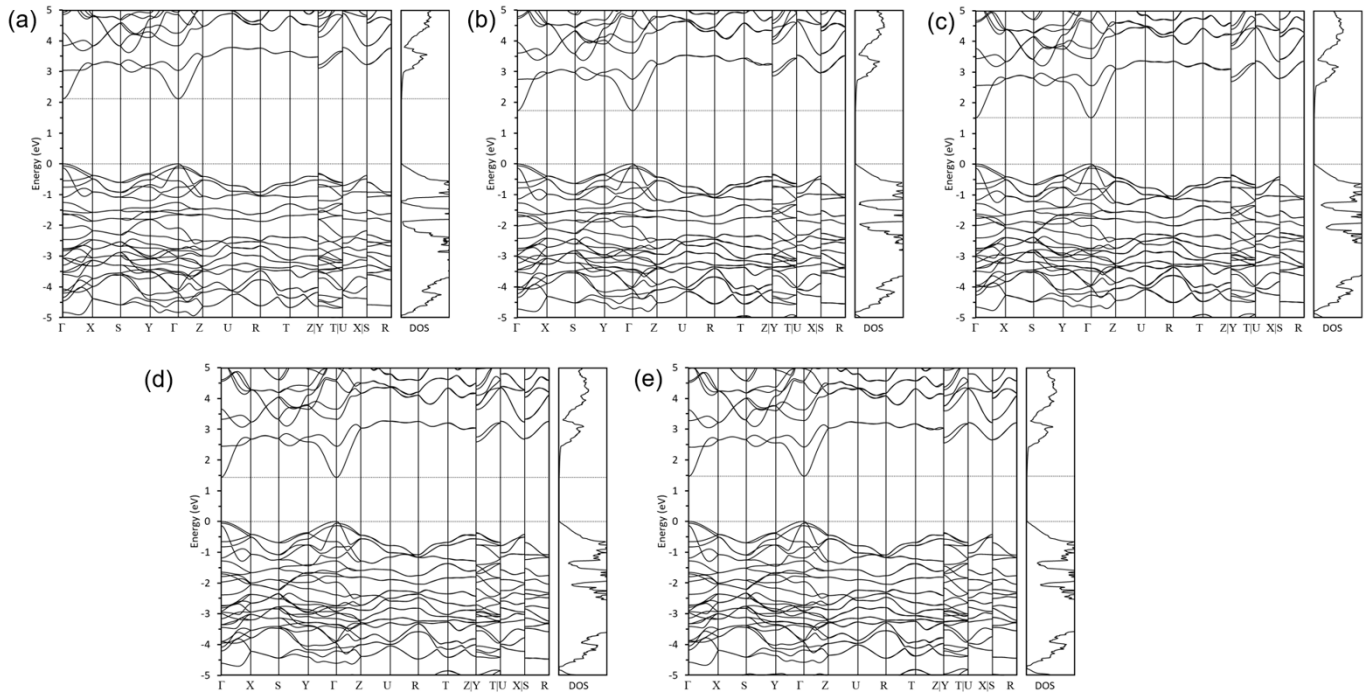

Figure S25. Electronic structures of different $CuZn_2InS_xSe_{4-x}$ compositions calculated using HSE06 hybrid functionals along with virtual crystal approximation. (a) $CuZn_2InS_4$, (b) $CuZn_2InS_3Se$, (c) $CuZn_2InS_2Se_2$, (d) $CuZn_2InSSe_3$, and (e) $CuZn_2InSe_4$.

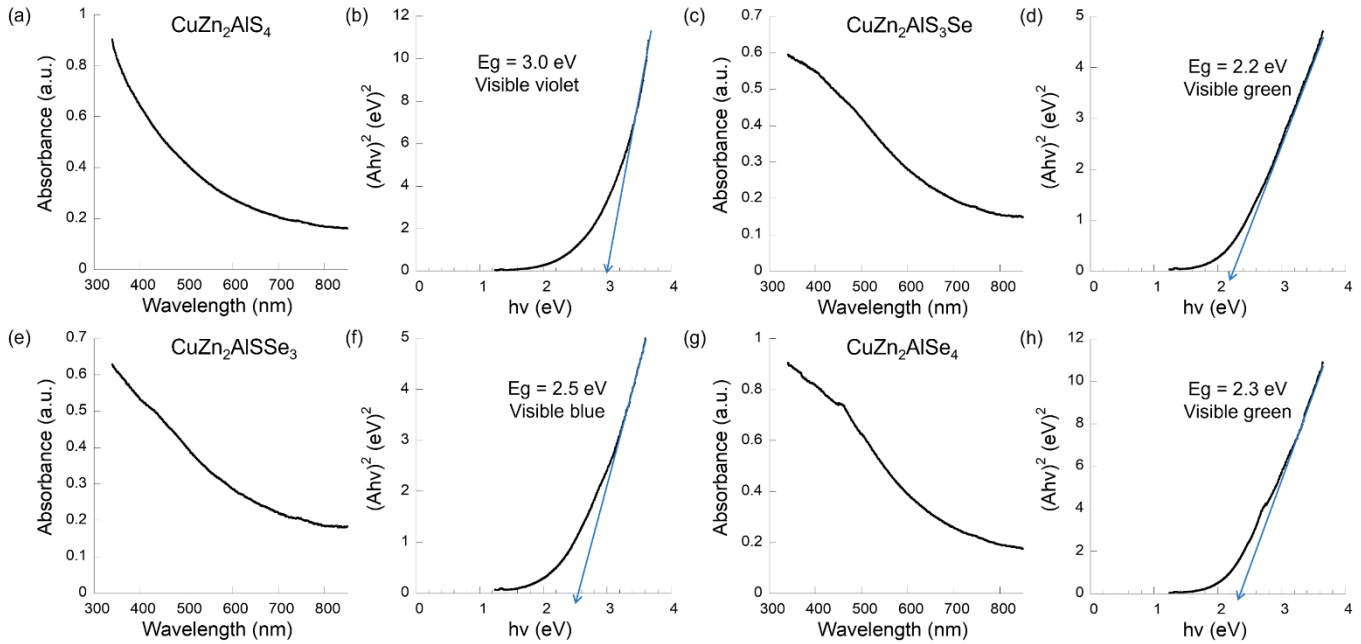

Figure S26. UV-vis and Tauc plots showing experimental bandgaps of $CuZn_2AlS_xSe_{4-x}$ nanocrystals. (a-b) $CuZn_2AlS_4$, (c-d) $CuZn_2AlS_3Se$, (e-f) $CuZn_2AlSSe_3$, and (g-h) $CuZn_2AlSe_4$.

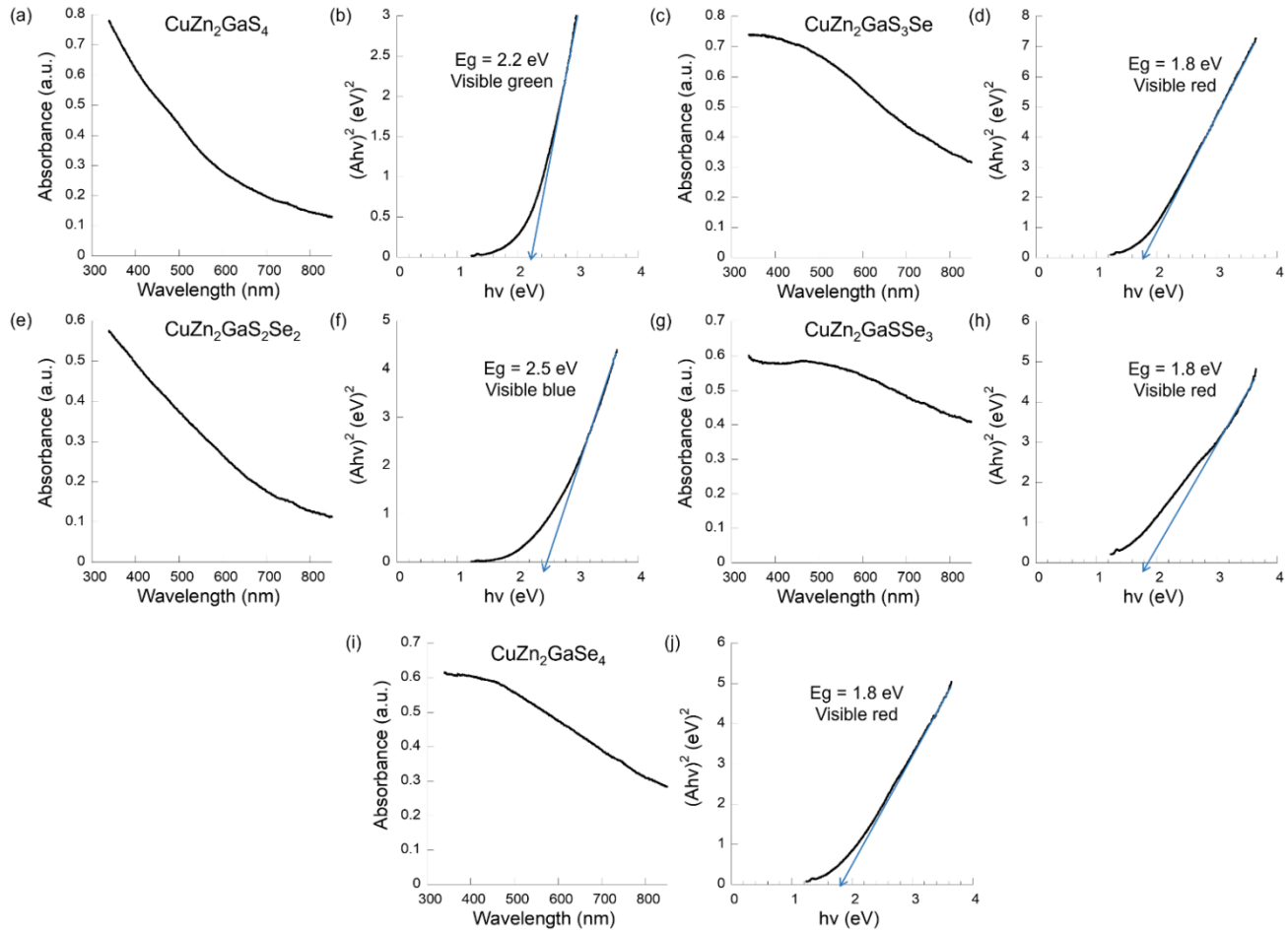

Figure S27. UV-vis and Tauc plots showing experimental bandgaps of $CuZn_2GaS_xSe_{4-x}$ nanocrystals. (a-b) $CuZn_2GaS_4$, (c-d) $CuZn_2GaS_3Se$, (e-f) $CuZn_2GaS_2Se_2$, (g-h) $CuZn_2GaSSe_3$, and (i-j) $CuZn_2GaSe_4$.

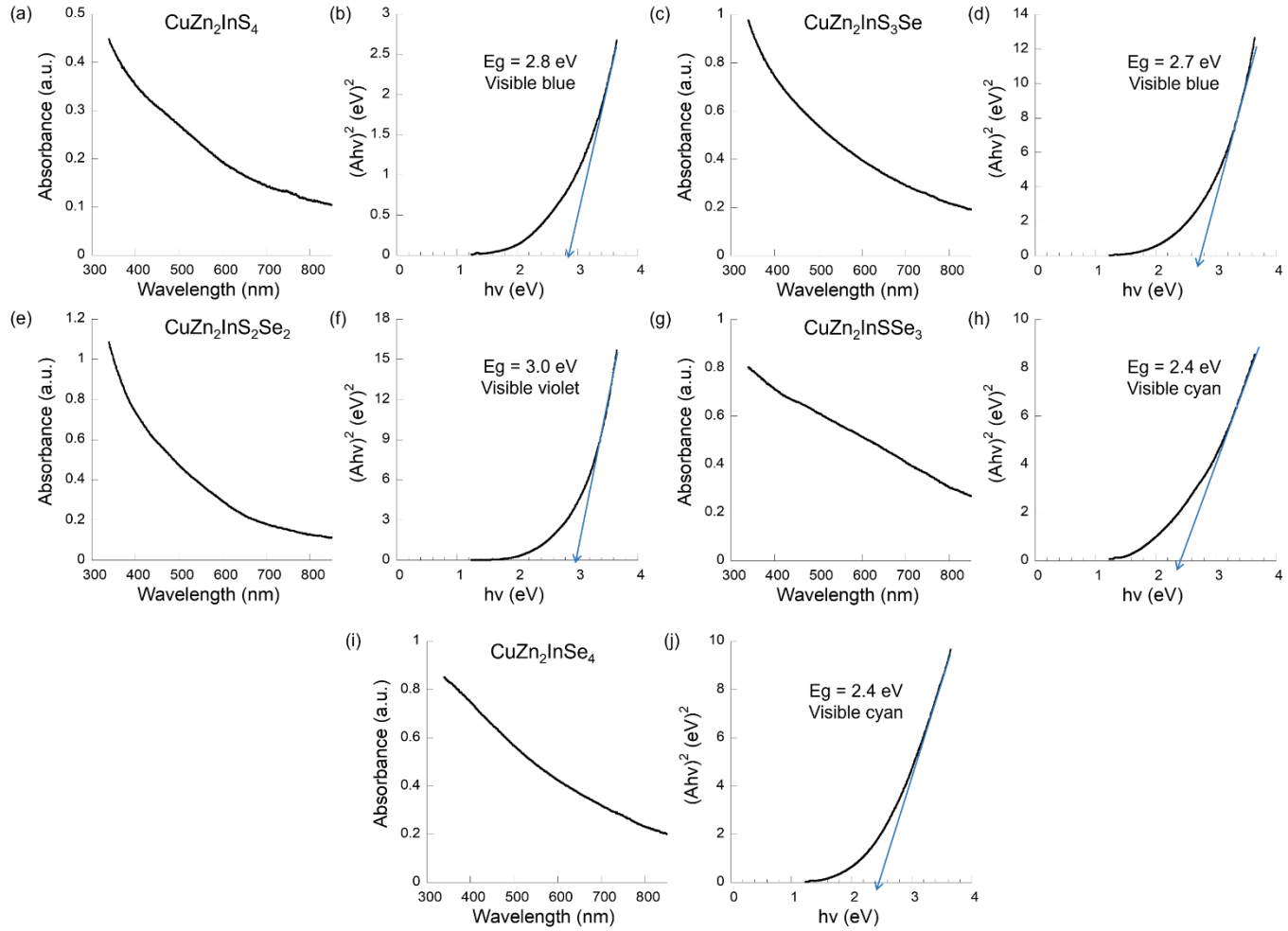

Figure S28. UV-vis and Tauc plots showing experimental bandgaps of $CuZn_2InS_xSe_{4-x}$ nanocrystals. (a-b) $CuZn_2InS_4$, (c-d) $CuZn_2InS_3Se$, (e-f) $CuZn_2InS_2Se_2$, (g-h) $CuZn_2InSSe_3$, and (i-j) $CuZn_2InSe_4$.

References

1 A. Ghosh, S. Palchoudhury, T. Rajalingam, Z. Zhou, N. Naghibolashrafi, K. Ramasamy and A. Gupta, *Chem. Commun.*, 2016, **52**, 264.
2 G. Kresse, *J. Non Cryst. Solids.*, 1995, **193**, 222.
3 G. Kresse and J. Furthmuller, *Phys. Rev. B*, 1996, **54**, 11169.
4 P.-E. Blochl, *Phys. Rev. B*, 1994, **50**, 17953.
5 G. Kresse and D. Joubert, *Phys. Rev. B*, 1999, **59**, 1758.
6 J. Sun, A. Ruzsinszky and J.-P. Perdew, *Phys. Rev. Lett.*, 2015, **115**, 036402.
7 L. Bellaiche and D. Vanderbilt, *Phys. Rev. B*, 2000, **61**, 7877.
8 J. Heyd, J.-E. Peralta, G.-E. Scuseria and R.-L. Martin, *J. Chem. Phys.*, 2005, **123**, 174101.
9 W. Setyawan and S. Curtarolo, *Comput. Mater. Sci.*., 2010, **49**, 299.